

CRITICAL PARAMETERS OF PEROVSKITE COMPOSITION $\text{Pr}_{5/8}\text{Ca}_{3/8}\text{Mn}_{0.9875}\text{Pd}_{0.0125}\text{O}_3$, EXHIBITING THE CROSSOVER OF FIRST AND SECOND ORDER PHASE TRANSITION

Le Viet Bau¹, Nguyen Thi Ngoc², Trinh Thi Huyen³

Received: 10 June 2022/ Accepted: 15 March 2023/ Published: April 2023

Abstract: A compound of $\text{Pr}_{5/8}\text{Ca}_{3/8}\text{Mn}_{0.9875}\text{Pd}_{0.0125}\text{O}_3$ with orthorhombic structure was fabricated using a sol-gel method. The critical parameters with $\beta=0.188(5)$ and $\gamma=1.005(3)$ calculated from the magnetic data around Curie temperature of 260 K are quite close to those of the tricritical mean field model. This indicates that the magnetic interaction in the compound is a combination of the long- and short-range interactions. It means the paramagnetic-ferromagnetic phase transition of $\text{Pr}_{5/8}\text{Ca}_{3/8}\text{Mn}_{7.9/8}\text{Pd}_{0.1/8}\text{O}_3$ compound is crossover of the first- and second-order phase transitions.

Keywords: Perovskite, critical parameters, phase transition.

1. Introduction

Perovskite materials with the general formula $\text{R}_{1-x}\text{M}_x\text{MnO}_3$ (R are rare earth elements and M are divalent alkaline ions) have been widely studied because of their potential applications. Many in-depth studies have focused on studying the effects of these materials such as magnetoresistance, magnetocaloric effect, thermoelectric effects, etc. [1-6]. Theoretical and experimental studies have suggested that double exchange interaction (DE), Jahn-Teller distortion effect, phase separation, etc.[7-9] are the main causes for the above effects. These effects occur the most strongly at temperatures near the ferromagnetic - paramagnetic phase transition. Therefore, it can be seen that the critical parameters in the phase transition can relate to these effects. The study of critical parameters in manganite materials thus is very important to design materials using in the fields of electronics, refrigeration technology, renewable energy, etc. The critical parameters allows to understand the micromagnetic interaction pattern in the materials. These parameters are determined by theoretical research and experimental results. Recent studies have shown that micromagnetic interaction in some manganites can obey a mean-field model with long-range order interactions with DE interaction models [10,11]. However, some studies reported that there are compounds with short-range order interaction according to the Heissenberg model [12,13] or 3D-Ising [14]. In addition, several studies determining the critical parameters are an overlap between the mean field and the Heissenberg models [15-17], or 3D Ising [18, 19] or tricritical-mean-field [20]. In this paper, we present the results of studying the critical parameters of the $\text{Pr}_{5/8}\text{Ca}_{3/8}\text{Mn}_{0.9875}\text{Pd}_{0.0125}\text{O}_3$ sample fabricated by sol-gel method.

¹ Chairman of University Council, Hong Duc University; Email: levietbau@hdu.edu.vn

² Faculty of Natural Sciences, Hong Duc University

³ Department of Postgraduate Training Management, Hong Duc University

2. Experiment

$\text{Pr}_{5/8}\text{Ca}_{3/8}\text{Mn}_{0.9875}\text{Pd}_{0.0125}\text{O}_3$ ceramic sample was fabricated by sol-gel method. The initial chemicals include $\text{La}(\text{NO}_3)_2$, $\text{Ca}(\text{NO}_3)_2$, $\text{Mn}(\text{NO}_3)_2$ and PdCl_2 with a purity of 99.99%. The sample had been preheated at 9800C for 3 h and sintered at 10500C for 4 h in air. The structural phase was determined by X-ray diffraction measurement. The results showed that the sample is single-phase structure with orthorhombic structure. Magnetic measurements were performed on a physical property measurement system (PPMS-6000).

3. Results and Discussion

Fig.1 presents the temperature dependence of magnetization on field-cooled (FC) and zero-field-cooled (ZFC) modes in a magnetic field of 100 Oe. It is clear that the sample behaves a ferromagnetic-paramagnetic phase transition at $T_C \sim 260$ K. The difference of the magnetization value in FC and ZFC modes at temperatures below T_C implies that the sample exhibits magnetic glassiness [21].

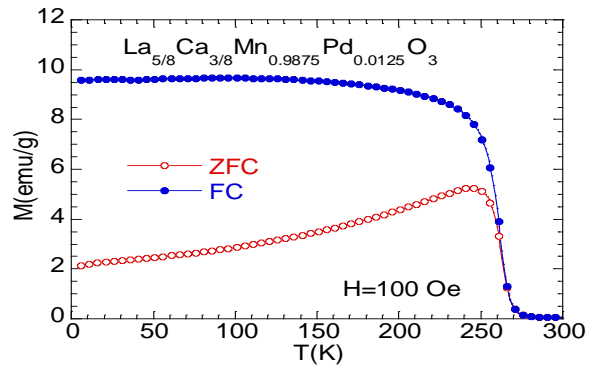


Fig.1. The temperature dependence of magnetisation measured in the ZFC and FC modes.

In order to explore the nature of phase transition in the sample, magnetic measurements of the applied magnetic dependence of magnetization at temperatures close to the T_C were performed. Isothermal $M(H)$ measurements are carried out in the temperature range of 219K-295K with step of 2K. The results are displayed in Fig.2.

As can be seen from the Fig.2, in the low temperature region, far from T_C , the magnetization value increases rapidly in the low magnetic field region. The increase decreases gradually and does not saturate but increases linearly in the high magnetic field. These signs suggest that the sample is not completely ferromagnetic, but possibly partly non-ferromagnetic, resulting in the linearity in the high magnetic field without saturation [8]. The value from the saturation of the ferromagnetic part

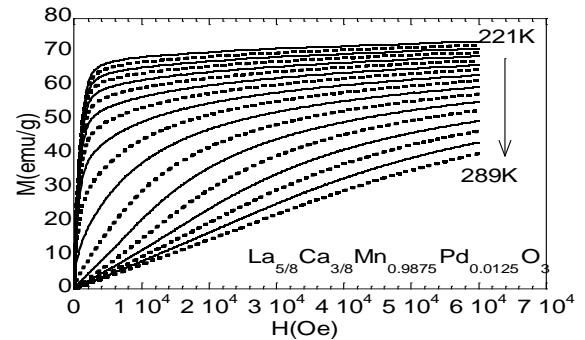


Fig.2. The applied field dependence of magnetisation in different temperatures

could be determined by extrapolating the $M(H)$ curve to the vertical axis. The slope of the linear part in the high magnetic field gives the value of the χ . As increasing the measurement temperatures, the saturation magnetisation value gradually decreases and rapidly decreases at the temperatures up to the ferromagnetic - paramagnetic phase transition. At high temperatures, the $M(H)$ curve is linear, showing the paramagnetic properties of the sample.

From the $M(H)$ curves at different temperatures, Arot curves are constructed assuming to agree with the theoretical models. Figure 3 shows the Arot curves according to the mean field (3a), 3D Heissenberg (3b), 3D Ising (3c) and Tricritical mean field (3d) models. If a model reflects the true nature of the sample, in the high applied field the Arot lines in the sufficiently high magnetic field will be parallel lines and the line measured at the transition temperature must pass through the origin. As can be seen from the Figure 3, there is not any model that can completely satisfy the above requirements. However, it can be found that the tricritical mean field model is the most suitable. Thus, the critical parameters of the sample can be seen close to the values of $\beta=0.25$ và $\gamma=1$.

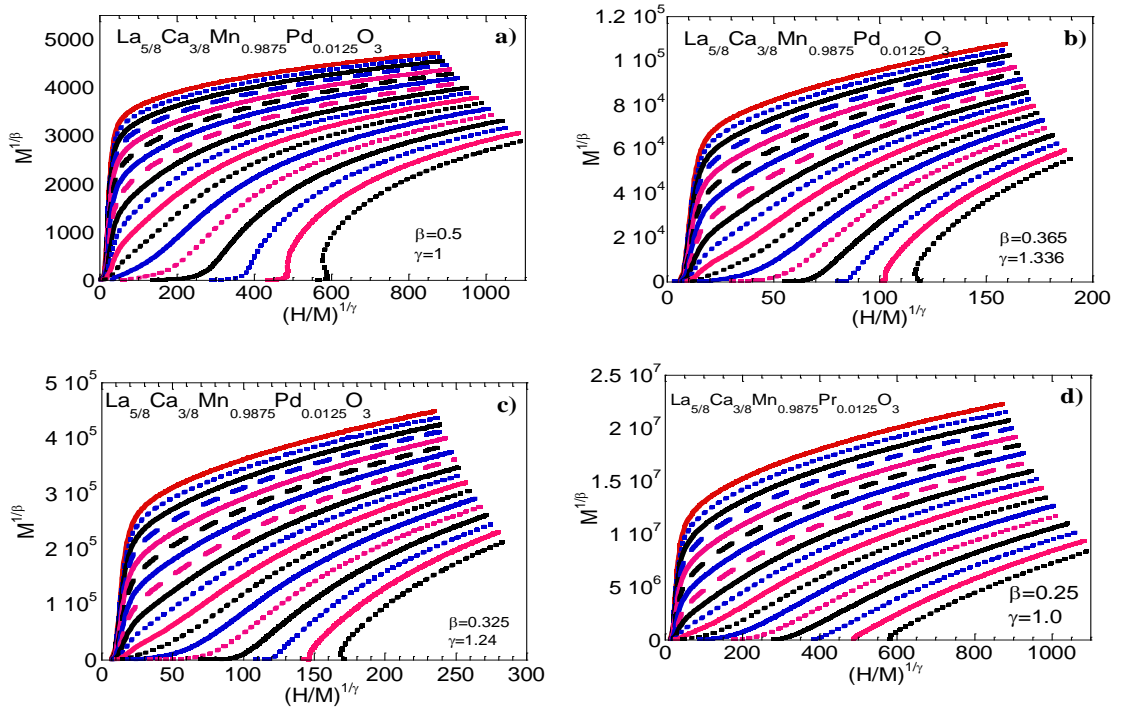


Fig.3. The Arott plots assumed to agree with the models of mean-field (a), Heisenberg (b), Ising (c) and tricritical-mean-field (d).

From the Arot curves, compared with the Banerjee criterion [22], we see that the ferromagnetic-paramagnetic phase transition of the sample is a second order phase transition. For the second-order phase transition, in the temperature range around T_C , the critical parameters related to the values from spontaneity and inductance can be determined from the expression [23]:

$$M_S(T) = M_0 |\varepsilon|^\beta, \quad \varepsilon < 0 \quad (1)$$

$$\chi^{-1}(T) = (h_0 / M_0) \varepsilon^\gamma, \quad \varepsilon > 0 \quad (2)$$

$$M = DH^{1/\delta}, \quad \varepsilon = 0 \quad (3)$$

Where, ε is the reduction of temperature, defined $(T-T_C)/T_C$, M_0 , h_0 and D are the critical values. β , γ , δ are the critical parameters corresponding to the spontaneous magnetic $M_S(T,0)$, initial inductance $\chi_0(T)$ and the critical isotherm magnetometer $M(T_C,H)$ respectively. The M_S value was extrapolated from the matched Arot curves. As mentioned above, the tricritical mean field model is the best fit. By extrapolating the curves to the vertical and horizontal axes to determine the M_S and χ_0 values, respectively, the values of the $M_S(T,0)$ and $\chi_0(T)$ are determined.

With the values of M_S and χ_0^{-1} matched according to the rules as in formulas (1) and (2), the values of β and γ will be determined. From these values the correct Arot curves are further constructed, the M_S and χ_0^{-1} values are further matched to obtain the values β and γ . Such a process is repeated until the values of β and γ are almost unchanged. With such an approach, after some execution, the M_S and χ_0^{-1} values are determined and the T_C , β and γ values obtained are $\sim 260.1(5)$, $0.227(7)$ and $1,008(7)$, respectively as shown in Fig.4.

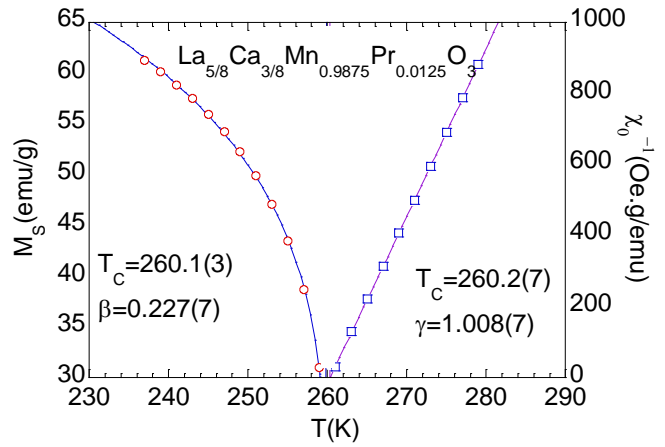


Fig.4. Spontaneous magnetisation, inverse initial susceptibility and critical parameters of the sample

With these critical values, the model interacts closer to the tricritical mean field model. Meanwhile, this model shows that the magnetic interaction is crossover of the first order phase transition and the second order phase transition. Therefore, equations (1) and (2) may no longer be accurate. In addition, the values of β and γ can be determined according to the Kouvel-Fisher law according to the formulas [24]:

$$\frac{M_s}{dM_s} = \frac{T - T_C}{\beta}, \quad T < T_C \quad (4)$$

$$\frac{\chi^{-1}}{d\chi^{-1}} = \frac{T - T_C}{T_C}, \quad T > T_C \quad (5)$$

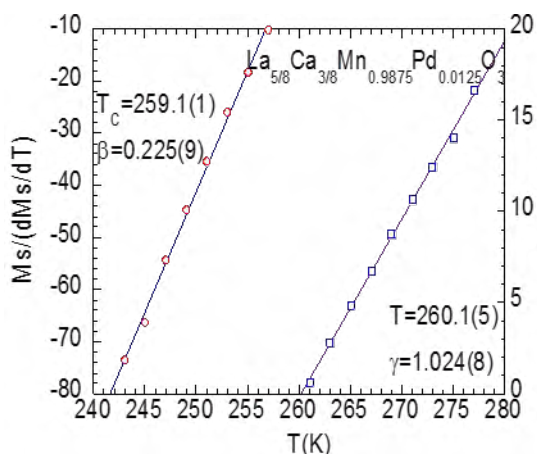


Fig.5. The critical parameters of the sample obtained by the Kouvel-Fisher method

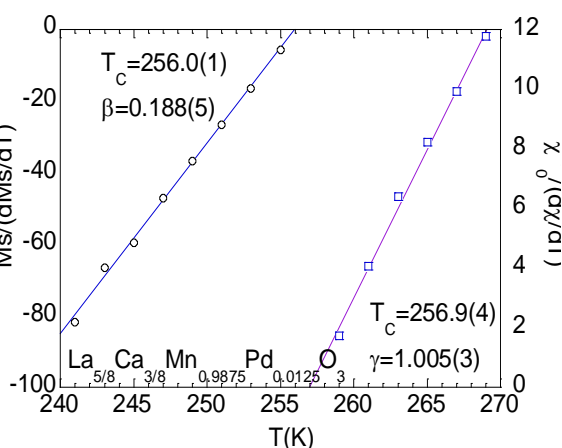


Fig.6. The last result of critical parameters of the sample after several caculation by the Kouvel-Fisher method

From these relations, the values of β and γ have been determined and shown in Fig.5. The temperature value is averaged of the matching results in the two regions above and below the phase transition temperature. As can be seen in Figure 5, the critical values obtained are $T_C=259.6(3)$, $\beta=0.225(9)$ and $\gamma=1.024(8)$. Comparing two pairs of values of β and γ obtained from two different methods, we find that the values are quite close to each other, indicating that the values can faithfully reflect the nature of the sample.

Similar to what was done with the MAP method, in order to determine the critical values more accurately, the correct Arot curves were re-built from the results in Figure 5. The relations (4) and (5) are applied to recalculate the T_C , β and γ values. The process is repeated until these values are almost unchanged and the result is as shown in Fig.6.

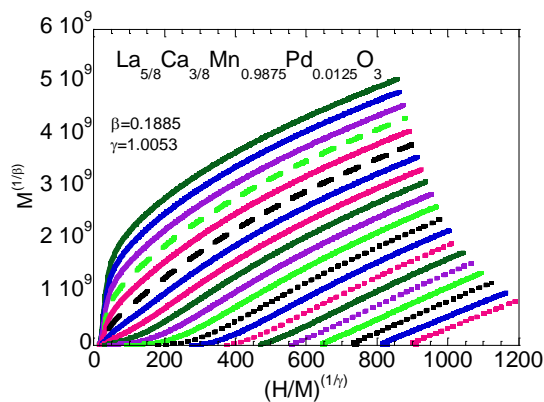


Fig.7. The Arott plots modified with the value of critical parameters added

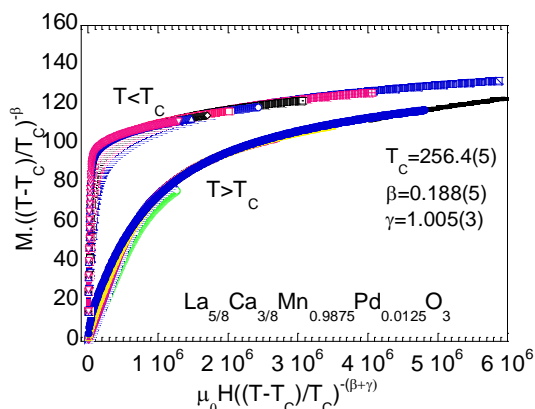


Fig.8. The series of M vs H according to the formular (6)

In order to be able to verify the accuracy of the critical values, Arot plot modified with defined critical values are reconstructed and displayed in Fig.7. As can be seen from the Fig.7, in the high applied field the Arot plots become parallel to each other and at the transition temperature ($\sim 256\text{K}$), the Arot line passes through the origin. This proves that the found critical values are quite accurate. Furthermore, the accuracy of these values can be verified by the family of lines representing the relationship between magnetisation and applied fields by the expression [25]:

$$M(\mu_0 H, \varepsilon) = \varepsilon^\beta f_{\pm}(H\alpha^{-(\beta+\gamma)}), \quad (6)$$

where f_+ and f_- are functions depending on the temperature range above and below T_C , respectively. If the critical values are correct, the curves that depend M on H according to expression (6) will belong to 2 separate branches above and below T_C . Fig.8 presents the curves showing the applied field dependence of magnetisation according to expression (6). As can be seen in the Figure 8, the curves representing expression (6) belong to 2 separate branches corresponding to above and below T_C very clearly. Therefore, it can be seen that the above critical values are reliable [26].

With the parameter set of $\beta = 0.188(5)$ and $\gamma = 1,005(3)$, it shows that the micromagnetic interaction model in the compound does not seem to fit any of 4 known theoretical models. The above results show that the sample $\text{Pr}_{5/8}\text{Ca}_{3/5}\text{Mn}_{0.9875}\text{Pd}_{0.0125}\text{O}_3$ exhibits magnetic heterogeneity in the material and the intersection between the first and second order phase transitions. This result is similar to some manganese materials which have similar composition such as $\text{Pr}_{0.63}\text{A}_{0.07}\text{Sr}_{0.3}\text{MnO}_3$ ($\text{A}=\text{Pr}, \text{Sm}$ and Bi) [20] or $\text{Pr}_{0.7}\text{Ba}_{0.1}\text{Sr}_{0.2}\text{MnO}_3$ [27]. This could be explored in effective exponents of perovskite with a structural phase transition from cubic-to-trigonal and cubic-to-tetragonal symmetry [28].

The value δ is then determined from expression (3). However, since there is no $M(H)$ curve at the correct phase transition temperature, this value is approximated from the $M(H)$ curve at 257K , which is close to the transition temperature $T_C=256.4(5)\text{K}$ as shown in Fig.9.

4. Conclusions

The critical values of the compound were calculated from the magnetic measurements. The set of critical parameters $T_C=2.564(5)\text{K}$, $\beta=0.188(5)$, $\gamma=1.005(3)$,

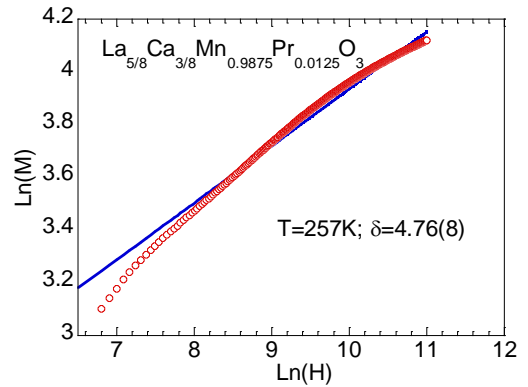


Fig.9. The value of δ obtained from $M(H)$ curve at 257K

$\delta=4.76(8)$ show that the micromagnetic interaction model in the material is the intersection between the interactions of short and long ranges. The ferromagnetic-paramagnetic phase transition is also the intersection between the first order phase transition and the second order phase transition.

References

- [1] P. Ramirez (1997), Colossal magnetoresistance, *J. Phys.: Condens. Matter.*, 9, p.8171.
- [2] M. H. Phan and S. C. Yu (2007), Review of the magnetocaloric effect in manganite materials, *Journal of Magnetism and Magnetic Materials*, 308, p.325.
- [3] S. Jin, T. H. Tiefel, M. McCormack, R. A. Fastnacht, R. Ramesh, L. H. Chen (1994), Thousandfold Change in Resistivity in Magnetoresistive La-Ca-Mn-O Films, *Science*, 264, p.413.
- [4] L. E. Hueso, P. Sande, D. R. Miguens, J. Rivas, F. Rivadulla, M. A. Lopez-Quintela (2002), Tuning of the magnetocaloric effect in $\text{La}_{0.67}\text{Ca}_{0.33}\text{MnO}_{3-\delta}$ nanoparticles synthesized by sol-gel techniques, *J. Appl. Phys.*, 91, p.9943.
- [5] L. V. Bau, N. M. An (2016), Magneto-electric properties and magnetic entropy change in perovskite $\text{La}_{0.7}\text{Sr}_{0.3}\text{Mn}_{1-x}\text{Ti}_x\text{O}_3$, *Journal of Magnetism and Magnetic Materials*, 420, 275-279.
- [6] C. Zener (1951), Interaction between the d-Shells in the Transition Metals, *Phys. Rev.* 82, 403-405.
- [7] J. B. Goodenough (1955), Theory of the Role of Covalence in Perovskite-Type Manganites $[\text{La}, \text{M}(\text{II})]\text{MnO}_3$, *Phys. Rev.* 100(2), 564-573.
- [8] E. Dagotto (2002) ,Nanoscale Phase Separation and Colossal Magnetoresistance, *Springer-Verlag, Berlin Heidelberg New York*.
- [9] L.V. Bau, N.V. Khiem, N.X. Phuc, L.V. Hong, D.N.H. Nam, P. Nordblad (2010), Observation of mixed-phase behavior in the Mn-doped cobaltite $\text{La}_{0.7}\text{Sr}_{0.3}\text{Co}_{1-x}\text{Mn}_x\text{O}_3$ ($x=0-0.5$), *Journal of Magnetism and Magnetic Materials*, 322, 753-755.
- [10] A. K. Pramanik, A. Banerjee (2009), Critical behavior at paramagnetic to ferromagnetic phase transition in $\text{Pr}_{0.5}\text{Sr}_{0.5}\text{MnO}_3$: A bulk magnetization study, *Phys. Rev. B* 79, 214426.
- [11] F. Ben Jemaa, S.H. Mahmood, M. Ellouze, E.K. Hlil, F. Halouani (2015), Structural, magnetic, magnetocaloric, and critical behavior of selected Ti-doped manganites, *Ceramics International*, 41(6), 8191-8202.
- [12] P.T. Phong, L.T.T. Ngan, L.V. Bau, N.M. An, L.T.H. Phong, N.V. Dang, and In-Ja Lee (2018), Critical Phenomena and Estimation of Spontaneous Magnetization by Magnetic Entropy Analysis of $\text{La}_{0.7}\text{Sr}_{0.3}\text{Mn}_{0.94}\text{Cu}_{0.06}\text{O}_3$, *Metallurgical and Materials Transactions A*, 49A, 385.
- [13] A.Tozri, R. Kamel, W.S. Mohamed, *et al.* (2022), Critical exponents and magnetic entropy change across the continuous magnetic transition in (La, Pr)-Ba manganites. *Appl. Phys. A* 128, 575.
- [14] Saoussen Mahjoub (2015), Mohamed Baazaoui, E.K. Hlil, Mohamed Oumezzine, Effect of synthesis techniques on structural, magnetocaloric and critical behavior of $\text{Pr}_{0.6}\text{Ca}_{0.1}\text{Sr}_{0.3}\text{Mn}_{0.975}\text{Fe}_{0.025}\text{O}_3$ manganites, *Ceramics International*, 41(9), Part B, 12407-12416.

- [15] Dinh Chi Linh, Nguyen Thi Viet Chinh, Nguyen Thi Dung, Le Viet Bau, Nguyen Huu Duc, Do Hung Manh, Tran Dang Thanh (2023), Critical behavior and room temperature magnetocaloric effect of La-doped $\text{Pr}_{0.7}\text{Sr}_{0.3}\text{MnO}_3$ compounds, *Physica B: Condensed Matter*, 661, 414945.
- [16] B. Padmanabhan, H. L. Bhat, S. Elizabeth, S. Rössler, U. K. Rössler, K. Dörr, and K. H. Müller (2007), Critical properties in single crystals of $\text{Pr}_{1-x}\text{Pb}_x\text{MnO}_3$, *Phys. Rev. B* 75, 024419.
- [17] R. Venkatesh, M. Pattabiraman, S. Angappane, G. Rangarajan, K. Sethupathi, Jessy Karatha, M. Fecioru-Morariu, R. M. Ghadimi, and G. Guntherodt (2007), Complex ferromagnetic state and magnetocaloric effect in single crystalline $\text{Nd}_{0.7}\text{Sr}_{0.3}\text{MnO}_3$, *Phys. Rev. B* 75, 224415,.
- [18] Sumei Li, Mingfang Shu, Meng Wang, Chengbing Pan, Gaochao Zhao, Lihua Yin, Wenhai Song, Jie Yang, Xuebin Zhu, Yupin Sun (2023), Critical behavior at paramagnetic to ferrimagnetic phase transition in A-site ordered perovskite $\text{CaCu}_3\text{Cr}_2\text{Nb}_2\text{O}_{12}$, *Physica B: Condensed Matter*, 648, 414376.
- [19] H. Ben Khelifa, R. M'nassri, S. Tarhouni, Y. Regaieg, W. Cheikhrouhou-Koubaa, N. Chniba-Boudjada, A. Cheikhrouhou (2018), Critical behaviour and field dependence of magnetic entropy change in K-doped manganites $\text{Pr}_{0.8}\text{Na}_{0.2-x}\text{K}_x\text{MnO}_3$ ($x = 0.10$ and 0.15), *Journal of Solid State Chemistry*, 257, 9-18.
- [20] A. Elghoul, A. Krichene, N. Chniba Boudjada, W. Boujelben (2018), Rare earth effect on the critical behavior of $\text{La}_{0.75}\text{Ln}_{0.05}\text{Sr}_{0.2}\text{MnO}_3$ manganites, *Ceramics International*, 44 (12), 14510-14517.
- [21] A. Elghoul, A. Krichene, W. Boujelben (2017), Landau theory and critical behavior near the ferromagnetic-paramagnetic transition temperature in $\text{Pr}_{0.63}\text{A}_{0.07}\text{Sr}_{0.3}\text{MnO}_3$ ($\text{A}=\text{Pr}, \text{Sm}$ and Bi) manganites, *Journal of Physics and Chemistry of Solids*, 108, 52-60.
- [22] Le Viet Bau, Nguyen Xuan Phuc, The-Long Phan, Seong-Cho Yu, and Per Nordblad(2006), Glassy ferromagnetism and frustration in $\text{La}_{0.7}\text{Ba}_{0.3}\text{Mn}_{0.7}\text{Ti}_{0.3}\text{O}_3$, *Journal of Applied Physics* 99, 08Q306.
- [23] S.K. Banerjee (1964), On a generalised approach to first and second order magnetic transitions, *Phys. Lett.* 12, 16.
- [24] A. Arrott (1957), Criterion for ferromagnetism from observations of magnetic isotherms, *Phys. Rev.* 108, 1394.
- [25] J.S. Kouvel and M.E. Fisher (1964), Detailed magnetic behavior of nickel near its Curie point, 136, 1626.
- [26] H.E. Stanley (1971), Introduction to Phase Transitions and Critical Phenomena (London: Oxford University Press,), 1-21.
- [27] P. Sarkar, T. Roy, N. Khan, P. Mandal (2020), Unconventional critical behavior in a Sm-based ferromagnetic: Effect of tricritical point, *Physica B*, 383, 412050.
- [28] Y. Pham, T.V. Manh, T.D. Thanh, D.S. Yang, S.C. Yu, H.H. Kim (2019), Magnetic and table-like magnetocaloric properties of polycrystalline $\text{Pr}_{0.7}\text{Ba}_{0.1}\text{Sr}_{0.2}\text{MnO}_3$, *Journal of Electronic Materials*, 48(10), 6583-6590.
- [29] Amnon Aharony, Ora Entin-Wohlman, Andrey Kudlis (2022), Different critical behaviors in perovskites with a structural phase transition from cubic-to-trigonal and cubic-to-tetragonal symmetry, *Physical Review B*, 105(10), 104101.